CHAPTER V
PREPARATION AND CHARACTERIZATION OF HIGH-SURFACE-AREA COPPER-CERIA-ZIRCONIA MIXED OXIDES PREPARED BY SOL-GEL PROCESS AND THEIR CATALYTIC ACTIVITIES FOR CO OXIDATION

5.1 Abstract

This work focused on copper-ceria-zirconia mixed oxides prepared through a surfactant-aid sol gel method at room temperature. The amount of ceria:zirconia is fixed at a 6:4 mole ratio, while the copper amount was varied, depending on the desired compositions. The surface features, textural properties, and crystalline structure of the mixed oxides were studied by means of Brunauer-Emmett-Teller specific surface areas measurement (BET), X-ray diffraction (XRD), Transmission electron microscopy (TEM), UV-visible diffuse reflectance spectroscopy (UV-DRS), and temperature programmed reduction (TPR). The results indicated that there are three copper species in the catalysts; namely, the finely dispersed CuO, the copper ion in the solid solution, and the bulk CuO. The catalyst with 25 mol% copper showed the highest catalytic activity for the CO oxidation reaction. Since the catalytic activity of the catalyst declined dramatically after the finely-dispersed CuO removal, the main active species for CO oxidation should be the finely-dispersed CuO species. The catalytic activity of all catalysts increased with increasing reaction temperature.

Keywords: Copper, Ceria, Zirconia, Sol-gel process, CO oxidation

5.2 Introduction

In recent years, a lot of catalysts have been developed for the catalytic oxidation of CO because of their many applications, such as pollution control devices for vehicle exhaust, CO gas sensors, gas purification of CO_2 lasers, and catalytic combustion[1]. Noble metals catalysts such as Pd, Pt, and Rh have been proved to be very effective for the CO oxidation reaction[2, 3]. Although these precious metal catalysts have high catalytic activity and high temperature stability, their high cost of noble metal may limit their applicability. Because of this problem, attention has been given to the cheap transitional metal oxide catalysts, especially copper oxide[4, 5]. During CO oxidation, copper-ceria mixed oxide catalysts can exhibit activities per unit surface area that are similar to those of noble-metal catalysts such as platinum[6]. The promoting effect has been correlated with the synergism of the redox properties of the system, which is achieved by the formation of copper–ceria interactions, with both components being significantly more readily reduced or oxidized than the corresponding independent components[7].

For CO oxidation, there are two factors that govern the activity of the CuO-CeO_2 catalysts, which are surface area and active sites of the catalyst. Although much attention is paid to the CuO-CeO_2 catalyst preparation, CuO-CeO_2 catalysts with surface areas higher than $60m^2/g$ synthesized at room temperature have rarely been reported. It is well known that a catalyst with higher surface area generally gives better catalytic activity because it can provide more active sites.

Since a major drawback of ceria is its low stability in high temperature ranges, as a support its use will result in a significant efficiency decrease of the catalysts due to loss of surface area of the support, sintering of active metals and deactivation of ceria under thermally harsh environments[8].

Many studies show the improvement of textural properties by introducing doping elements in the CeO_2 fluorite-type lattice, and the most efficient metal seem to be zirconia. Adding zirconia to ceria-based catalysts not only improves the thermal stability

but also improves the redox properties of the active species, which is an important property in catalytic activity as discussed by our previous works[9, 10].

Mart´ınez-Arias *et al. s*tudied the catalytic activity of $CuO_x/Ce_{0.5}Zr_{0.5}O_2$ mixed oxides for CO oxidation reaction in the presence of NO. They proposed that two basic factors affecting the catalytic activity of this system are the facility for achieving a partially reduced state for the copper oxide phase at the interfacial zone and the redox properties of the $CuO_x/Ce_{0.5}Zr_{0.5}O_2$ interface[11].

Hongliang Chen *et al.* studied the CO oxidation reaction over $CuO/Ce_{0.5}Zr_{0.5}O_2$ catalysts. In their work, the $Ce_{0.5}Zr_{0.5}O_2$ solid solution was synthesized by a microwave-assisted solution-phase heating method and was then used as the support for a series of $CuO/Ce_{0.5}Zr_{0.5}O_2$ catalysts. They suggested that there are two kinds of copper species in the system, dispersed and crystalline, and that the active species, the dispersed form, should be mainly on the surface and/or in the form of small particles of the copper oxide species[12].

Despite many studies on the copper-ceria-zirconia solid solution mentioned above, it is believed that the CuO species are the active sites for CO oxidation, but the nature of the interaction between the active species and the supports is still unclear and widely open to study.

In this work, a series of high-surface-area nanosized Cu-Ce-Zr catalysts were prepared by sol-gel method at ambient temperature and their catalytic activity was tested for CO oxidation reaction. The copper species in the catalyst were distinguished, and the main active phase for CO oxidation was investigated.

5.3 Experimental

5.3.1 Materials

Cerium(IV)hydroxide, zirconium(IV) hydroxide, $Cu(CH_3COO)_2{\cdot}H_2O$, and sodium dodecyl sulfate were purchased from Aldrich Chemical Co. Inc. (USA) and used as received. Ethylene glycol was purchased from Farmitalia Carlo Erba

(Barcelona), and sodium hydroxide was purchased from Merck Company Co. Ltd. (Germany) and used as received. Triethylenetetramine was purchased from Facai Polytech. Co. Ltd. (Bangkok, Thailand) and distilled under vacuum (0.1 mm Hg) at 130°C prior to use.

5.3.2 Instruments

The Brunauer-Emmett-Teller (BET) specific surface areas of all powder samples were determined by N_2 adsorption and desorption isotherms at 77 K using a Quantachrome Corporation Autosorb. Prior to analysis, the samples were outgassed at 250°C for 4 h.

The structure of the samples was investigated from the wide-angle X-ray diffraction (XRD) on a D/MAX 2000 Rigaku using CuK$\propto$ radiation (λ = 1.5406 Å). The intensity data were collected at 25°C over a 2θ range of 5-90 degree. Lattice parameters of samples were considered in the case of cubic symmetry and were calculated by using the Vegard rule (a and c are the lattice parameters):

$$a_{average} = (2(\sqrt{2}a)+c)/3$$

The average grain size (D) was estimated according to the Scherrer equation:

$$D = 0.94\lambda / \beta \cos\theta$$

where θ is the diffraction angle of the (111) peak of the cubic phase or the (101) peak of the tetragonal phase, and β is the full width at half-maximum (fwhm) of the (111) or the (101) peak (in radian). The total metal content of all catalysts were confirmed by the inductive coupled plasma atomic emission spectroscopy technique.

Transmission electron microscopy (TEM) observations were made using a JEM-2100 JEOL (Japan) microscope.

UV-visibleible diffuse reflectance (UV-DRS) was obtained with a Shimazu UV-2550 spectrometer. The reflectance output from the instrument was converted using the Kubelka-Munk algorithm.

The reduction properties of the catalysts were measured by temperature programmed reduction (TPR). A Micromeritics TPD/TPR 2900 was employed as the analyzer for the temperatures of the thermal conductivity, using a furnace temperature up to 900°C at a linear ramp rate of 2.5°C/min. The sample was pretreated by flowing He over the sample at 120°C for 4 h and then cooled to room temperature before analysis; 10 mg of the catalysts were used for each test. The reaction mixture was consisted of 5% H_2 in N_2. An effluent gas stream from the reactor was first dehumidified by a cold water-trap before auto-sampling in a gas chromatograph (Agilent Technologies 6890N model). The results were recorded by Agilent Chemstation software. The observed peaks were identified by comparison with the retention time of the standard gas.

5.3.3 Precursor synthesis

The synthesis of the cerium glycolate complex and the sodium tris(glycozirconate) complex followed Wongkasemjit's work[13]. The cerium glycolate complex was prepared by making a mixture of cerium hydroxide (5.3 mmol of CeO_2), 18 ml of ethylene glycol and 5 mmol of triethylenetetramine with sodium hydroxide at about 12 mol% equivalents to cerium hydroxide. The mixture was magnetically stirred and heated to the boiling point of ethylene glycol for 18 h under N_2. The reaction mixture was cooled overnight under N_2. The precipitated product was filtered and washed with acetonitrile, followed by drying under vacuum.

A similar process was used to synthesize the sodium tris(glycozirconate) complex. Zirconium hydroxide (11.4 mmol of ZrO_2) and approximately 200 mol% sodium hydroxide equivalent to the zirconium dioxide were suspended in 35 ml of ethylene glycol. The reaction mixture was heated under nitrogen in a thermostatted oil bath at 200°C. After 12 h, the solution was virtually clear, indicating reaction completion. The reaction mixture was cooled, and 2-5% of dried methanol in acetonitrile was added. The product precipitated out as a white solid. The solid was filtered off, washed with acetonitrile, and dried under vacuum.

5.3.4 Catalysts Preparation

The catalysts with various copper content were prepared via surfactant-aided sol gel technique by dissolving cerium glycolate, sodium tris(glycozirconate), $Cu(CH_3COO)_2 \cdot H_2O$, and sodium dodecyl sulfate in a 2 M NaOH solution. The amount of Ce:Zr:sodium dodecyl sulfate:NaOH was fixed at a mole ratio of 6:4:1:2.5, while the copper content was varied, depending on the desired compositions. The mixture was stirred for 2 h to obtain a gel and was then kept at room temperature for 10 days. After the aging step, the gels were washed three times with deionized water to remove the sodium content generated from the sodium tris(glycozirconate), the free surfactant, and the NaOH added during the gelation step. The samples were then put in an oven at 110°C overnight before calcination at 500°C for 2 h in air.

5.3.5 Catalytic Activity Measurement

The catalytic activity of the CO oxidation for the synthesized samples was evaluated in a differential packed-bed quartz U-tube reactor (ID 6 mm). The inlet gas consisted of 1% CO and 1% O_2 balanced in N_2 with the total flow rate of 80 mL/min corresponding to the space velocity of 120,000 $mLg^{-1}h^{-1}$ and the gas was directly exposed to the 25 mg catalyst as the reactor temperature was stabilized at the reaction temperature without any pretreatment. The reaction temperature was monitored by a thermocouple placed in the middle of the catalyst bed. The effluent gas from the reactor was analyzed by auto-sampling in an on-line gas chromatograph.

For reaction temperature comparison, the reaction was carried out using 25 mg of catalyst at 100 and 120°C with a space velocity of 300,000 $mLg^{-1}h^{-1}$.

5.4 Results and Discussion

5.4.1 Brunauer-Emmett-Teller specific surface areas measurement (BET)

In this work, a series of copper-ceria-zirconia catalysts with a copper content of 10 to 40 mol% was prepared. Surface area, pore size, and pore volume for the

samples being calcined at 500°C for 2 h are listed in Table 5.1. It should be noted here that the minimum calcination temperature in this work was 500°C. At this temperature, all the organic residues were removed and detected using TGA (not shown).

From the BET data, it can be seen that with an increase of copper amount from 10 to 40 mol%, the surface areas of the catalysts decrease from 201 to 105 m^2/g, the pore sizes increase from 6.5 to 12 nm, whereas the pore volume decrease from 0.41 to 0.11 nm. The dependence of pore size and pore volume on the amount of copper in the samples is consistent with that of the BET surface area. The decreased BET surface areas consequently increased pore sizes and decreased pore volume, possibly due to the formation of the CuO when increasing the copper amount in the samples[14].

5.4.2 X-ray diffraction (XRD)

The calculated lattice parameters according to the Vegard rule for a series of copper-ceria-zirconia catalysts with various amounts of copper are also listed in Table 5.1. The cell parameters of the copper-ceria-zirconia samples were smaller than that of ceria-zirconia mixed oxide prepared by same method (0.528 nm), which is in good agreement with the product of ceria-zirconia mixed oxide obtained from other route[12]. The decrease in lattice parameters of the copper-ceria-zirconia samples provided evidence that some Cu^{2+} ions are incorporated into the ceria and zirconia lattice to form the Cu-Ce-Zr solid solutions. Since the radius of Cu^{2+} ions (0.072 nm) is smaller than that of Ce^{4+} (0.097 nm) and Zr^{4+} ions (0.084 nm), when part of the CuO incorporates into the fluorite lattice and Cu^{2+} replaces Ce^{4+} or Zr^{4+} a reduction in the cell parameter of sample occurs. These results indicate that the Cu-Ce-Zr solid solution was formed in the samples[15]. The lattice parameter was not significantly changed with increasing copper content. Considering the size differences between the ionic radius of Cu^{2+} and those of Ce^{4+} and Zr^{4+}, a strong decrease in the lattice parameter should be expected with the increase in Cu^{2+} ions substitution in the fluorite lattice. But, simultaneously, an increase in the oxygen vacancy is promoted for the substitution of Ce^{4+} or Zr^{4+} with Cu^{2+} ions; therefore, only a small decrease in lattice parameter is observed[16].

The wide-angle XRD patterns of the mixed oxides are illustrated in Figure 5.1. No distinguishing peaks of well-known crystalline CuO (2θ = 35.5 and 38.7°) appear in 10-25 mol% copper-content samples, which confirms that the Cu-Ce-Zr solid solution was formed in the samples. However, it cannot be ruled out that the CuO particles might be highly dispersed on the Ce-Zr surfaces, which are undetectable as a consequence of sensitivity and size limits of the XRD technique[17].

The characteristic peaks of crystalline CuO were investigated and the intensity of these peaks increase with increasing copper amount in the samples from 30 to 40 mol%, indicating the formation of an additional phase, attributed to the monoclinic CuO[16]. In addition, all of the samples prepared by sol-gel method in this work have a calculated particle size lower than 5 nm, according to the Debye-Scherrer equation.

5.4.3 Transmission electron microscopy (TEM)

The TEM images of the samples with 25 mol% copper content are displayed in Figure 5.2. The samples show a foam-like structure, resulting from closely aggregated metal oxide nanoparticles[17]. The particle size is around 5 nm, which is in good agreement with the crystal size obtained from XRD.

5.4.4 UV-visible diffuse reflectance spectroscopy (UV-DRS)

The UV-visible spectra of the copper-ceria-zirconia catalysts with various amounts of copper are shown in Figure 5.3. The spectra of the catalysts show strong absorption bands at 250-280, 340 nm and a large absorption band at 600-800 nm. According to literature,[18-22] the band at 250-280 nm indicates the $O^{2-} \longrightarrow Cu^{2+}$ ligand-to-metal charge-transfer (LMCT) transition, where the Cu ions occupy isolated sites over the support. The band at 340 nm indicates the formation of $(Cu\text{-}O\text{-}Cu)^{2+}$ clusters in a highly dispersed state, which is not detectable by XRD. The large absorption band at 600-800 nm is assigned to $^2E_g \longrightarrow {}^2T_{2g}$ transitions of Cu^{2+} situated in the distorted octahedral symmetry. Since the samples were calcined and the spectra measured in air, the existence of Cu^+ species was less likely[22].

With the increase of copper content, the intensity of the absorption in the 600-800 nm range increased, and the absorption band between 250 and 280 nm decreased with copper amount, showing an increase of crystalline and bulk CuO[19]. This was consistent with the observation that the intensities of the XRD peaks increased with the increase of copper loading.

5.4.5 Temperature programmed reduction (TPR)

The TPR profiles of the samples with various copper amounts are shown in Figure 5.4. Large differences in the reduction profiles between catalysts with different copper amounts suggest that the state of the copper significantly changes as the copper amount changes. These TPR profiles also indicate that the distribution of the copper species strongly depends on the amount of copper in the samples, as described in the XRD and UV-DRS results.

Two low-temperature reduction peaks (α and β), which occur below 200°C, can be detected from all of the samples. The intensity of the α and β peaks initially increased and the peak positions shift to lower temperatures with increasing copper content up to 25 mol%. With further increase in copper content in the sample the intensity of these two peaks remain constant.

Overbury *et al.* suggested that ceria-zirconia mixed oxide is known to be reducible, but the degree of reduction is low for temperatures less than 200°C and the copper-promoted reduction of Ce^{4+} to Ce^{3+} in copper-ceria catalysts with Cu/Ce < 0.5 occurs mainly above 200°C[23], so the observed reduction peaks at temperatures lower than 200°C should be mainly due to the reduction of copper species[24]. The reduction peaks of copper-ceria-zirconia catalysts are much lower than that of pure copper oxide, which is characterized by a single peak at 380°C reported in literature[25], indicating that the reducibility of the copper species in the Cu-Ce-Zr mixed oxides is enhanced.

Since XRD and UV-DRS results indicate the coexistence of the Cu-Ce-Zr solid solutions and the highly dispersed CuO on the Ce-Zr surface in every sample, the

low-temperature reduction peaks (α and β) should be due to the reduction of these two copper species.

Huber *et al.*[24] interpreted that the reducibility of single copper atoms incorporated in the Ce-Zr mixed oxides bulk could be lower than that of surface copper or copper particles due to accessibility and/or stability of the oxide state, which is in accordance with results obtained by Ramaswamy *et al.*[26] for nanocrystalline Cu-Zr oxides. They found the extra-lattice species to be reduced more easily than the framework-substituted ions. Additionally, Wrobel *et al.*[27] reported the Cu clusters in Cu-Ce oxides to be more reducible than isolated Cu^{2+} ions.

Luo *et al.*[25] suggested that the highly dispersed CuO in catalyst can be easily removed by immersing the sample in a nitric acid solution. In this present work, a catalyst with 25 mole% copper content was immersed in concentrated nitric acid (12 ml HNO_3/g catalyst) for 40 h and then filtered, washed with deionized water, and dried at 120°C overnight.

After the acid treatment, the CuO content was decreased from 24.5 to 12.3 mol% by ICP analysis. This indicates that a large number of copper atoms in the catalyst were removed by this process. The BET surface area increase from 129 to 150 m^2/g indicates that the removal of CuO enhanced the surface area. This was corresponding to the observation that the surface area decreases with the increase of copper content because of the CuO formation. However, the cell parameter and crystallite size were not visibly changed compared to the untreated sample.

The H_2-TPR profiles for catalysts with 25 mol% copper content before and after acid treatment are shown in Figure 5.5. The lower temperature peak (at about 150°C) almost disappears after the acid treatment, indicating that the finely dispersed CuO species can be removed by acid treatment and also shows that the α peak is represented by highly dispersed CuO, while the β peak is represented by Cu^{2+} incorporating into the solid solution.

Therefore, we propose that peak α is mainly due to the reduction of highly dispersed CuO species on the surface of solid solution, while peak β is mainly

due to the reduction of the copper ion in the solid solution or a little larger bulk CuO particle.

A new peak at approximately 270°C, namely γ, can be observed from the samples with 30-40 mol% copper content and is attributed to large three-dimensional clusters. As the copper content increases, the γ peak becomes broad and shifts to high temperature, which might be due to an increase in crystallinity and size of the CuO with an increase of copper amount, as evidenced from XRD results, because the reduction temperature of the smaller crystalline CuO particles is lower than that of the larger crystalline CuO particles due to the promotion of the support[12]. It is clear that the larger γ peak area of the TPR and the larger signal intensity of CuO peaks in XRD are observed with higher copper-content samples.

On the basis of these observations, the TPR results suggest the presence of three different CuO species, which are the finely dispersed CuO, the copper ion in the solid solution, and the bulk CuO species. This interpretation of copper species incorporated in the Ce-Zr mixed oxide is in accordance with results obtained by Luo *et al.*[14, 28].

5.4.6 CO oxidation

The catalytic activities of CO oxidation over a series of catalysts are shown in Figure 5.6. The results show that the temperature for 90% conversion of CO, namely T_{90}, of the samples decreases sharply with increasing copper content from 10 to 25 mol%. The lowest T_{90} is 80°C, which is achieved from the 25 mol% copper-content sample. When increasing the copper content from 25 to 40 mol%, T_{90} increases, indicating a catalytic activity decrease. From these, it can be concluded that increasing the copper content cannot always promote catalytic activity.

With respect to the BET surface area of the 25 mol% copper-content sample being similar to that of 30 mol%, this phenomenon is related to the status of copper in the composite. Results from XRD and TPR for the 30 mol% copper-content sample show larger and crystallized CuO particles, so in this sample there will be less

interfacing between the copper and the support, compared with the 25 mol%, and also a lack of active sites at the interface. Moreover, bulk CuO, which is known as an insulator and contributes very little to the total active area can prevent the gas molecules from accessing the active site, causing the decrease in catalytic activity of the sample[29].

It is commonly believed that the finely dispersed CuO on the surface of solid solution is the active phase for CO oxidation[30]; therefore, the catalytic activity should decrease if the active species is removed. From Figure 5.6 the 25 mol% copper-content catalyst with acid treatment shows a dramatic catalytic activity decrease, compared to the untreated one, indicating that finely dispersed CuO species are the main active species for the CO oxidation reaction.

The effects of reaction temperature on the activity of all catalysts are listed in Figure 5.7. When the reaction temperature is increased from 100 to 120°C, the CO conversion increases about four times. It can be concluded that the catalytic activity of the copper-ceria-zirconia catalysts for the CO oxidation is greatly influenced by reaction temperature.

When the catalysts, therefore, contain an appropriate amount of copper, Cu-Ce-Zr synergism in the reaction can be obtained; but if the copper content exceeds the optimum value, the formation of bulk CuO occurs and might cover the active species, which are mainly the finely dispersed CuO species, resulting in a catalytic activity decrease. From these experimental conditions the optimal copper content is around 25 mol%.

5.5 Conclusions

Copper-ceria-zirconia catalysts with various amounts of copper have been prepared via the surfactant-aided sol-gel process at ambient temperature and were tested for CO oxidation reaction. Three different CuO species, which are highly dispersed CuO, copper ion in the solid solution, and bulk CuO species, were distinguished by UV-DRS, XRD and TPR results. The highly dispersed CuO species are the active phase for

CO oxidation, since the activity of the catalyst declined after the removal of the highly dispersed CuO species by acid treatment.

5.6 Acknowledgments

The authors gratefully acknowledge the financial support of the Postgraduate Education and Research Program in Petroleum and Petrochemical Technology, Thailand, the PPT Consortium (ADB) Fund, Thailand, and the Ratchadapisake Sompote Fund, Chulalongkorn University. Special thanks go to Mr. Robert Wright for the English proofreading.

5.7 References

1. Min K, Song MW, Lee CH. *Appl. Catal. A* 2003; 251: 143.
2. Mariño F, Descorme C, Duprez D, *Appl. Catal. B* 2004 54: 59.
3. Costa CN, Christou SY, Georgiou G, Efstathiou AM. *J. Catal.* 2003; 219: 259.
4. Huang TJ, Yu TC, Chang SH. *Appl. Catal.* 1989; 52: 157.
5. Huang TJ, Yu TC. *Appl. Catal.* 1991; 72: 275.
6. Hummer JK. *Prog. Energy Combust. Sci.* 1980; 6: 177.
7. Martínez-Arias A, Fernández-García M, Soria J, Conesa JC. *J. Catal.* 1999; 182:367.
8. Kaˇspar J, Fornasiero P, Graziani M. *Catal. Today* 1999; 50: 285.
9. Rumruangwong M, Wongkasemjit S. *Appl. Organometal. Chem.* 2006; 20: 615.
10. Rumruangwong M, Wongkasemjit S. *Appl. Organometal. Chem.* 2008; 22: 1.
11. Martínez-Arias A, Fernández-García M, Hungria AB, Iglesias-Juez A, Galvez O, Anderson JA, Conesa JC, Soria J, Munuera G, *J. Catal.* 2003; 214: 261.
12. Hongliang C, Haiyang Z, Yong W, Fei G, Lin D, Junjie Z, *J. Mol. Catal. A: Chem.* 2006; 255: 254.
13. Ksapabutr B, Gulari E, Wongkasemjit S. *Mater. Chem. and Phy.* 2004; 83: 34.
14. Meng-Fei L, Jing-Meng M, Ji-Qing L, Yu-Peng S, Yue-Juan W. *J. Catal.* 2007; 246: 52.

15. Liang Q, Wu X, Weng D, Lu Z. *Catal Commu.* 2008;9: 202.
16. Fuerte A, Valenzuela RX, Daza L. *J. of Power Sources* 2007; 169: 47.
17. Lu C, Worrell WL, Vohs JM, Gorte RJ. *J. Electrochem. Soc.* 2003; 150: 1357.
18. Jeon G, Chaung J. *Appl. Catal.* 1994; 115: 29.
19. Komandur VRC, Guggilla VS, Dhachapally N, Kottapalli KS, Bojja S. *J. Phys. Chem. B* 2005; 109: 9437.
20. Chen L, Horiuchi T, Osaki T, Mori T. *Appl. Catal, B* 1999; 23: 259.
21. Velu S, Suzuki K, Okazaki M, Kapoor M P, Osaki T, Ohashi F. *J. Catal.* 2000; 194: 373.
22. Xiangxin Y, Larry EE, Keith LH. *Ind. Eng. Chem. Res.* 2006; 45: 6169.
23. Overbury SH, Huntley DR, Mullins DR, Glavee GN. *Catal. Lett.* 1998; 51: 133.
24. Huber F, Venvik H, Rønning M, Walmsley J, Holmena A. *Chem. Eng. J.* Article in press.
25. Meng-Fei L, Yi-Jun Z, Xian-Xin Y, Xiao-Ming Z. *Appl. Catal. A: General* 1997; 162: 121.
26. Ramaswamy V, Bhagwat M, Srinivas D, Ramaswamy AV. *Catal. Today* 2004; 97: 63.
27. Wrobel G, Lamonier C, Bennani A, D'Huysser A, Aboukais A, *J. Chem. Soc. Faraday Trans.* 1996; 92: 2001.
28. Meng-Fei L, Yu-Peng S, Ji-Qing L, Xiang-Yu W, Zhi-Ying P. *J. Phys. Chem. C* 2007; 111: 12686.
29. Shen W, Dong X, Zhu Y, Chen H, Shi J Micropor. Mesopor. Mater. 2005; 85: 157.
30. Luo MF, Zhong YJ, Yuan XX, Zheng XM. *Appl. Catal. A* 1997; 162: 121.

Table 5.1 Physical properties of copper-ceria-zirconia mixed oxide catalysts

Sample name	BET surface area (m^2/g)	Pore size (nm)	Pore volume (cc/g)	Lattice Parameter (nm)
10 mol % copper content	201	6.5	0.41	0.523
15 mol % copper content	186	7.2	0.36	0.522
20 mol % copper content	170	8.6	0.30	0.521
25 mol % copper content	154	9.8	0.26	0.521
30 mol % copper content	138	10.9	0.20	0.521
35 mol % copper content	120	11.5	0.16	0.521
40 mol % copper content	105	12.0	0.11	0.521

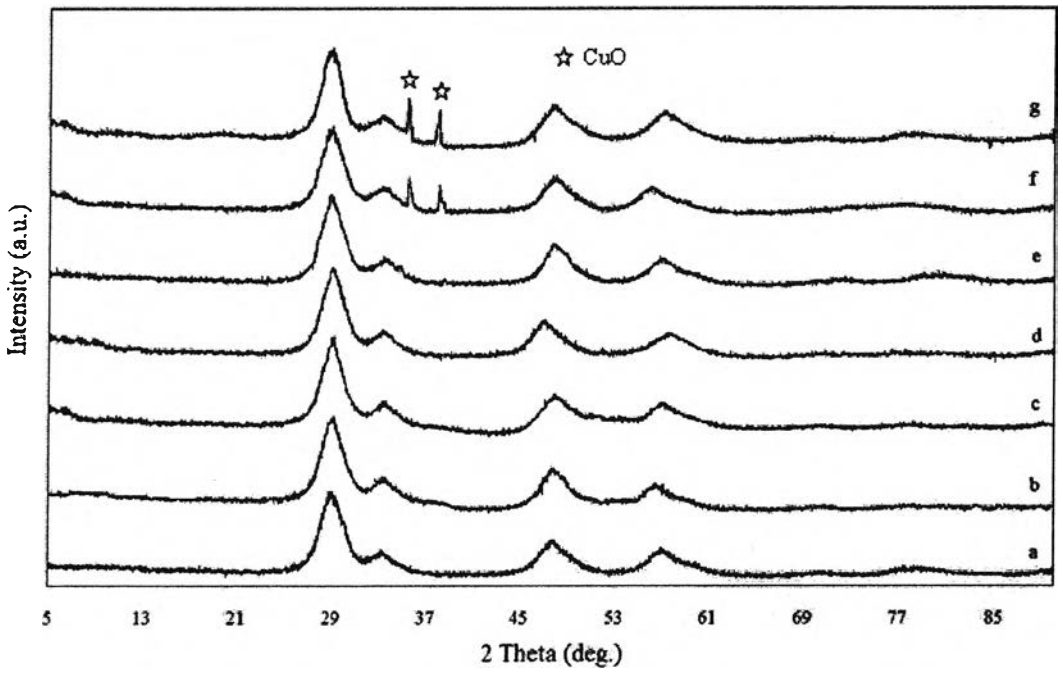

Figure 5.1 XRD patterns for mixed oxides with copper amounts of: (a) 10 mol%; (b) 15 mol%; (c) 20 mol%; (d) 25 mol%; (e) 30 mol%; (f) 35 mol%; and (g) 40 mol%.

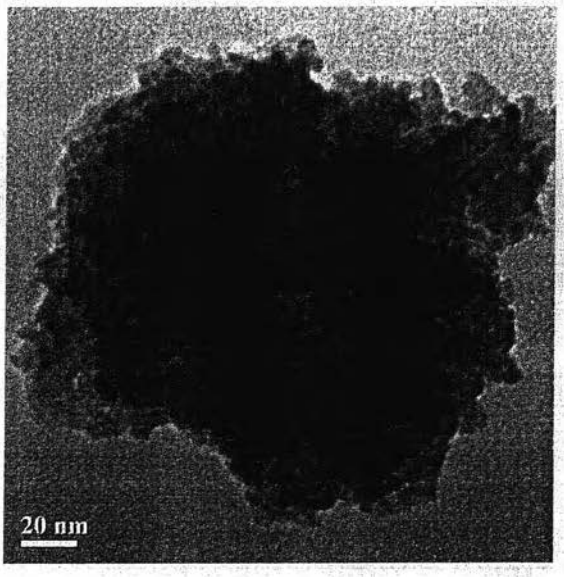

Figure 5.2 TEM image of the catalyst with 25 mol% copper content.

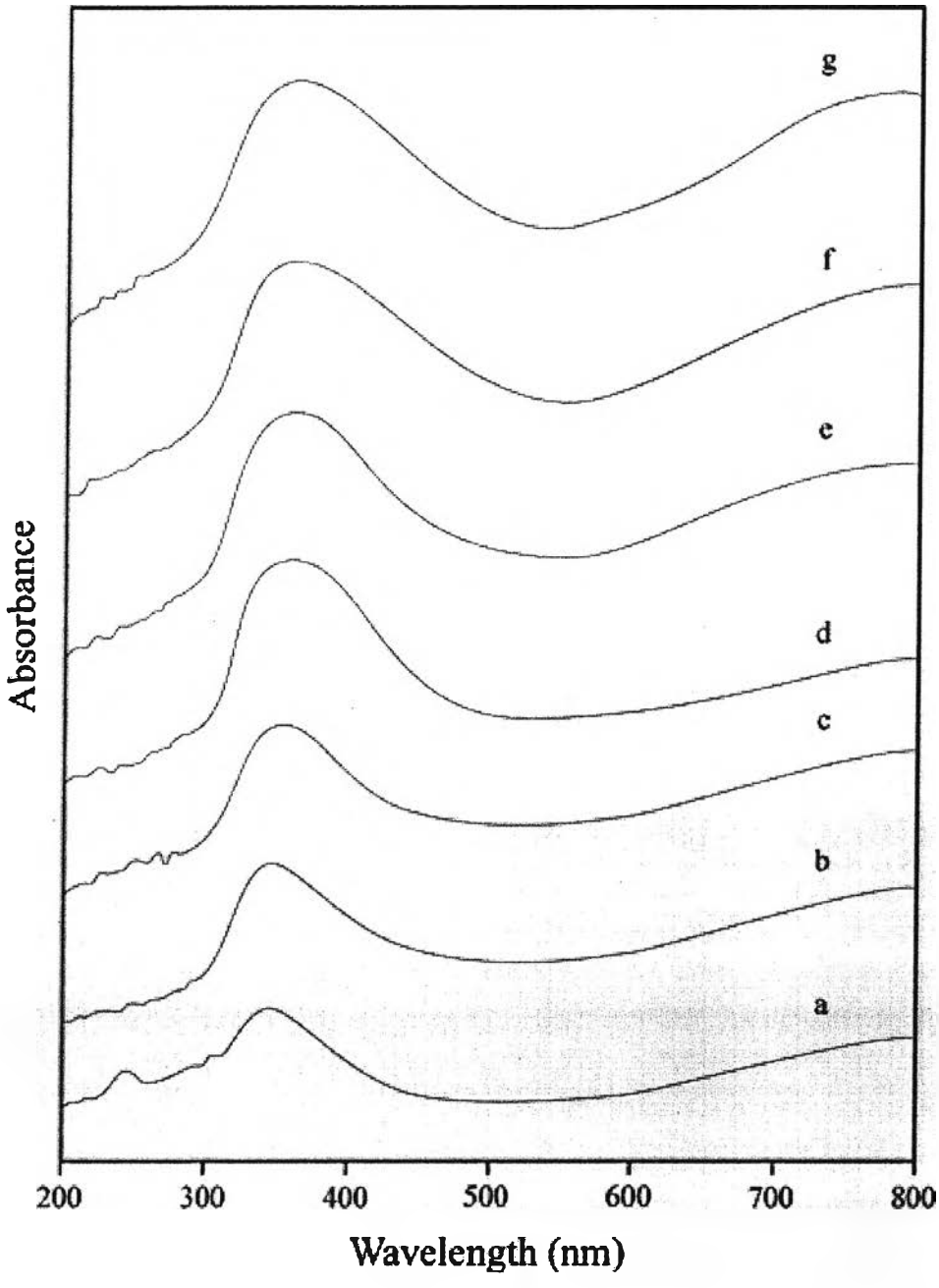

Figure 5.3 UV-visible spectra for mixed oxides with copper amounts of: (a) 10 mol%; (b) 15 mol%; (c) 20 mol%; (d) 25 mol%; (e) 30 mol%; (f) 35 mol%; and (g) 40 mol%.

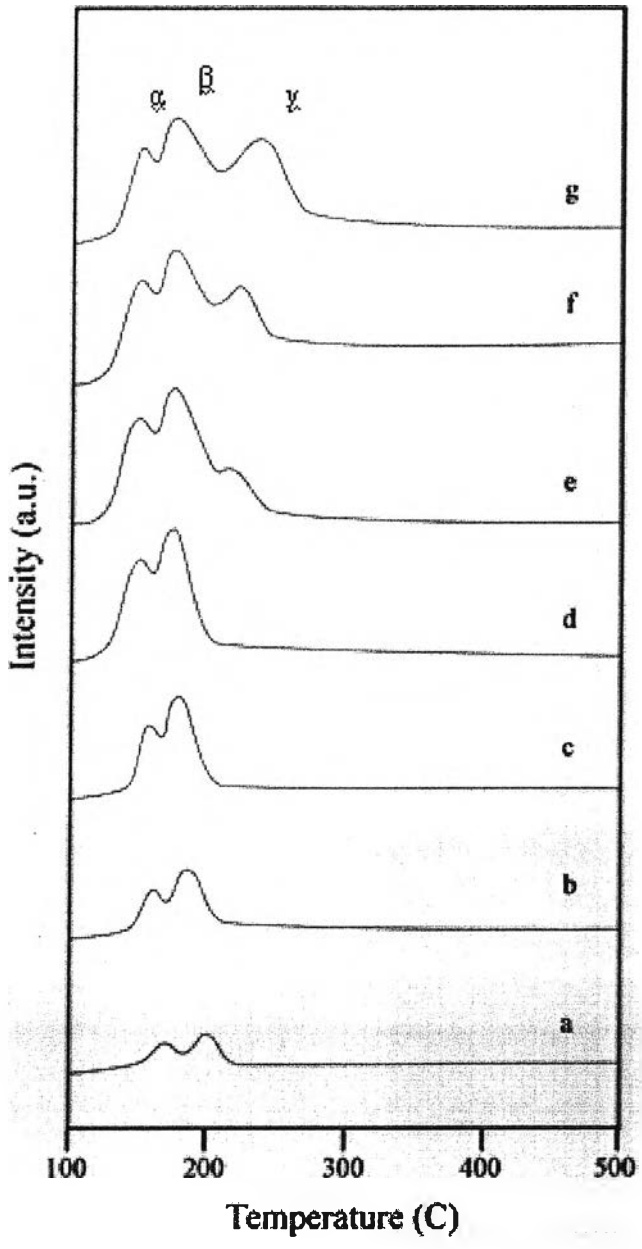

Figure 5.4 TPR profiles for mixed oxides with copper amounts of: (a) 10 mol%; (b) 15 mol%; (c) 20 mol%; (d) 25 mol%; (e) 30 mol%; (f) 35 mol%; and (g) 40 mol%.

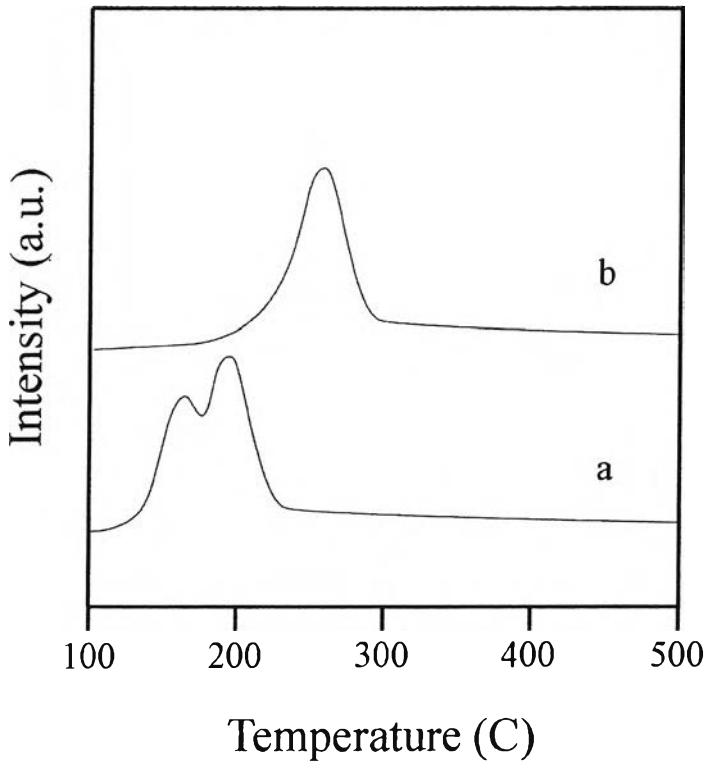

Figure 5.5 TPR profiles for mixed oxides with copper amounts of 25 mol%: (a) untreated and (b) H_2NO_3 treated.

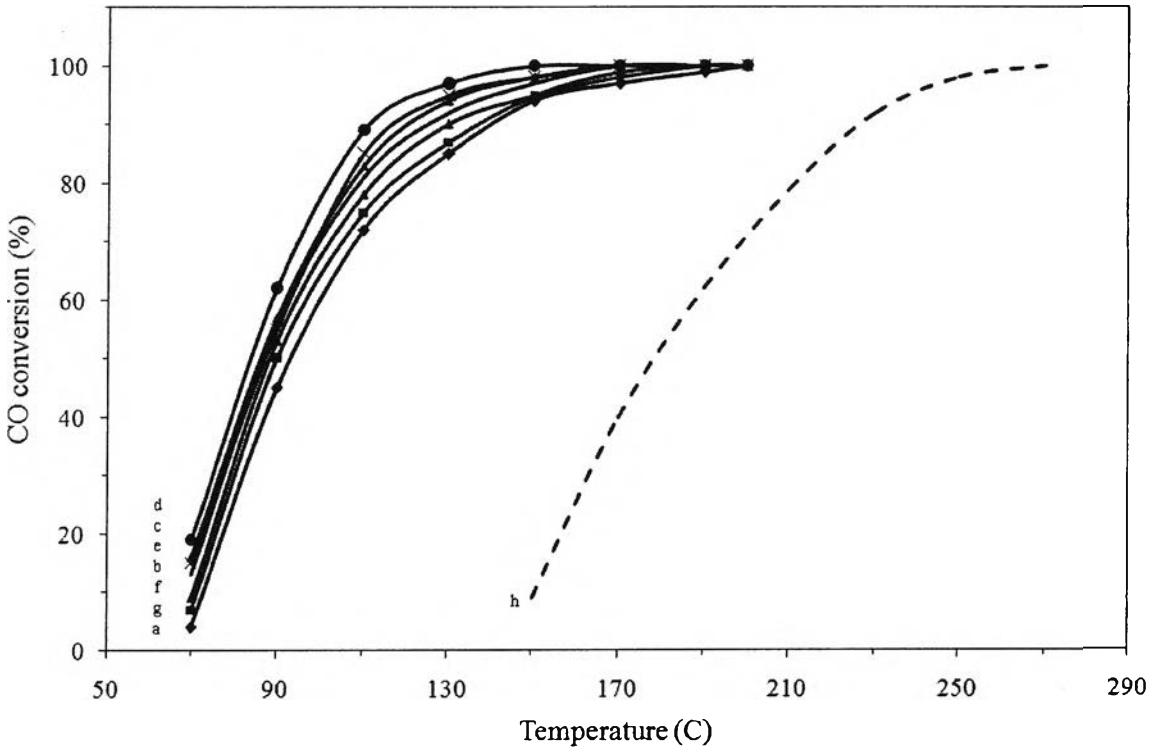

Figure 5.6 Catalytic activities of CO oxidation over copper mixed oxides with copper amounts of (a) 10 mol%; (b) 15 mol%; (c) 20 mol%; (d) 25 mol%; (e) 30 mol%; (f) 35 mol%; and (g) 40 mol%; (h) 25 mol% and H_2NO_3 treated.

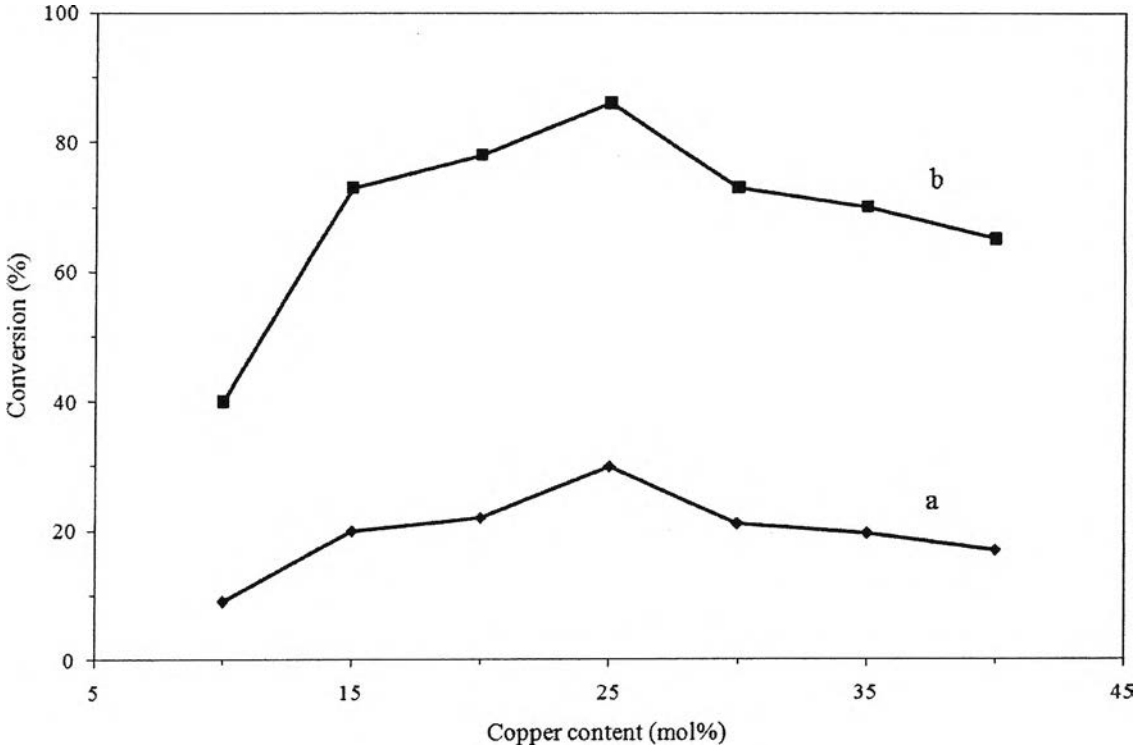

Figure 5.7 Catalytic activities of CO oxidation over copper mixed oxides at different temperatures: (a) 100°C and (b) 125°C.